Optical gap formation and localization properties of optical modes in deterministic aperiodic photonic structures

Svetlana V. Boriskina,* Ashwin Gopinath, and Luca Dal Negro

Department of Electrical and Computer Engineering, Boston University, Boston, MA, 20036, USA
**Corresponding author: sboriskina@gmail.com*

Abstract: We theoretically investigate the spectral and localization properties of two-dimensional (2D) deterministic aperiodic (DA) arrays of photonic nanopillars characterized by singular continuous (Thue-Morse sequence) and absolutely continuous (Rudin-Shapiro sequence) Fourier spectra. A rigorous and efficient numerical technique based on the 2D Generalized Multiparticle Mie Theory is used to study the formation of optical gaps and the confinement properties of eigenmodes supported by DA photonic lattices. In particular, we demonstrate the coexistence of optical modes with various degrees of localization (localized, extended and critical) and show that in-plane and out-of-plane optical energy confinement of extended critical modes can be optimally balanced. These results make aperiodic photonic structures very attractive for the engineering of novel passive and active photonic devices, such as low-threshold microlasers, sensitive detectors and bio-chemical sensors.

OCIS codes: (160.5298) Photonic crystals; (290.4210) Multiple scattering; (260.5740) Resonance; (170.4520) Optical confinement and manipulation.

References and links

1. C. Rockstuhl, U. Peschel, and F. Lederer, "Correlation between single-cylinder properties and bandgap formation in photonic structures," Opt. Lett. **31**, 1741–1743 (2006).
2. K. Mnaymneh and R. C. Gauthier, "Mode localization and band-gap formation in defect-free photonic quasicrystals," Opt. Express, **15**, 5089–5099 (2007), http://www.opticsinfobase.org/abstract.cfm?URI=oe-15-8-5089.
3. A. Della Villa, S. Enoch, G. Tayeb, V. Pierro, V. Galdi, and F. Capolino, "Band gap formation and multiple scattering in photonic quasicrystals with a Penrose-type lattice," Phys. Rev. Lett. **94**, 183903 (2005).
4. Y. Wang, X. Hu, X. Xu, B. Cheng, and D. Zhang, "Localized modes in defect-free dodecagonal quasiperiodic photonic crystals," Phys. Rev. B **68**, 165106 (2003).
5. Z. Feng, X. Zhang, Y. Wang, Z.-Y. Li, B. Cheng, and D.-Z. Zhang, "Negative refraction and imaging using 12-fold-symmetry quasicrystals," Phys. Rev. Lett. **94**, 247402 (2005).
6. E. Di Gennaro, C. Miletto, S. Savo, A. Andreone, D. Morello, V. Galdi, G. Castaldi, and V. Pierro, "Evidence of local effects in anomalous refraction and focusing properties of dodecagonal photonic quasicrystals," Phys. Rev. B **77**, 193104 (2008).
7. X. Xu, H. Chen, and D. Zhang, "Enhancement of stimulated emission in 12-fold symmetric quasi-crystals," Appl. Phys. B **89**, 29–34 (2007).
8. M. Notomi, H. Suzuki, T. Tamamura, and K. Edagawa, "Lasing action due to the two-dimensional quasiperiodicity of photonic quasicrystals with a Penrose lattice," Phys. Rev. Lett. **92**, 123906 (2004).
9. E. Macia, "The role of aperiodic order in science and technology," Rep. Prog. Phys. **69**, 397–441 (2006).
10. L. Dal Negro, N.-N. Feng, and A. Gopinath, "Electromagnetic coupling and plasmon localization in deterministic aperiodic arrays," J. Opt. A: Pure Appl. Opt. **10** 064013 (2008).
11. M. Dulea, M. Johansson, and R. Riklund, "Localization of electrons and electromagnetic waves in a deterministic aperiodic system," Phys. Rev. B **45**, 105–114 (1992).
12. W. Gellermann, M. Kohmoto, B. Southerland, and P. C. Taylor, "Localization of light waves in Fibonacci dielectric multilayers," Phys. Rev. Lett. **72**, 633 (1993).

#101449 - $15.00 USD Received 11 Sep 2008; revised 17 Oct 2008; accepted 17 Oct 2008; published 30 Oct 2008

13. L. Dal Negro, C. J. Oton, Z. Gaburro, L. Pavesi, P. Johnson, A. Lagendijk, R. Righini, M. Colocci, and D. S. Wiersma, "Light transport through the band-edge states of Fibonacci quasicrystals," Phys. Rev. Lett. **90**, 055501 (2003).
14. L. Dal Negro, M. Stolfi, Y. Yi, J. Michel, X. Duan, L. C. Kimerling, J. LeBlanc, and J. Haavisto, "Photon band gap properties and omnidirectional reflectance in Si/SiO_2 Thue-Morse quasicrystals," Appl. Phys. Lett. **84**, 5186–5188 (2004).
15. L. Dal Negro, J. H. Yi, Y. Yi, V. Nguyen, J. Michel, and L. C. Kimerling, "Spectrally enhanced light emission from aperiodic photonic structures," Appl. Phys. Lett., **86**, 261905, 2005
16. S. Chakraborty, M. C. Parker, and R. J. Mears, "A Fourier (k-) space design approach for controllable photonic band and localization states in aperiodic lattices," Photon. Nanostruct. Fundam. Appl. **3**, 139–147 (2005).
17. A. Gopinath, S. V. Boriskina, N.-N. Feng, B. M. Reinhard, and L. Dal Negro, "Photonic-plasmonic scattering resonances in determinsitic aperiodic structures," Nano Lett. **8**, 2423–2431 (2008).
18. L. Moretti and V. Mocella, "Two-dimensional photonic aperiodic crystals based on Thue-Morse sequence," Opt. Express, **15**, 15314–15323 (2007), http://www.opticsinfobase.org/abstract.cfm?URI=oe-15-23-15314.
19. S. V. Boriskina, A. Gopinath, and L. Dal Negro, "Optical gaps, mode patterns and dipole radiation in two-dimensional aperiodic photonic structures," Physica E (in the press), doi:10.1016/j.physe.2008.08.039.
20. J. D. Joannopolous, S. Johnson, R. D. Meade, and J. N. Winn, *Photonic crystals: Molding the flow of light* (Princeton University, Princeton, 2008).
21. S. Assefa, P. T. Rakich, P. Bienstman, S. G. Johnson, G. S. Petrich, J. D. Joannopoulos, L. A. Kolodziejski, E. P. Ippen, and H. I. Smith, "Guiding 1.5 μm light in photonic crystals based on dielectric rods," Appl. Phys. Lett. **85**, 6110–6112 (2004).
22. M. Tokushima, H. Yamada, and Y. Arakawa, "1.5-μm-wavelength light guiding in waveguides in square-lattice-of-rod photonic crystal slab," Appl. Phys. Lett. **84**, 4298–4300 (2004).
23. D. N. Chigrin, S. V. Zhukovsky, A. V. Lavrinenko, and J. Kroha, "Coupled nanopillar waveguides optical properties and applications," Phys. Status Solidi A **204**, 3647–3661 (2007).
24. S. Xiao and N. A. Mortensen, "Highly dispersive photonic band-gap-edge optofluidic biosensors," J. Europ. Opt. Soc. **1**, 06026 (2006).
25. P. S. Nunes, N. A. Mortensen, J. P. Kutter, and K. B. Mogensen, "Photonic crystal resonator integrated in a microfluidic system," Opt. Lett. **33**, 1623–1625 (2008).
26. S. V. Boriskina and L. Dal Negro, "Sensitive label-free biosensing using critical modes in aperiodic photonic structures," Opt. Express **16**, 12511-12522 (2008), http://www.opticsinfobase.org/abstract.cfm?URI=oe-16-17-12511.
27. C. S. Ryu, G. Y. Oh, and M. H. Lee, "Extended and critical wave functions in a Thue-Morse chain," Phys. Rev. B **46**, 5162–5168 (1992).
28. L. Kroon, E. Lennholm, and R. Riklund, "Localization-delocalization in aperiodic systems," Phys. Rev. B **66**, 094204 (2002).
29. L. Kroon and R. Riklund, "Absence of localization in a model with correlation measure as a random lattice," Phys. Rev. B **69**, 094204 (2004).
30. M. Dulea, M. Johansson, and R. Riklund, "Localization of electrons and electromagnetic waves in a deterministic aperiodic system," Phys. Rev. B **45**, 105–114 (1992).
31. D. Felbacq, G. Tayeb, and D. Maystre, "Scattering by a random set of parallel cylinders," J. Opt. Soc. Am. A **11**, 2526–2538 (1994).
32. A. A. Asatryan, K. Busch, R. C. McPhedran, L. C. Botten, C. Martijn de Sterke, and N. A. Nicorovici, "Two-dimensional Green's function and local density of states in photonic crystals consisting of a finite number of cylinders of infinite length," Phys. Rev. E **63** 046612 (2001).
33. S. V. Pishko, P. Sewell, T. M. Benson, and S. V. Boriskina, "Efficient analysis and design of low-loss WG-mode coupled resonator optical waveguide bends," J. Lightwave Technol. **25**, 2487–2494 (2007).
34. Y. Lai, Z.-Q. Zhang, C.-H. Chan, and L. Tsang, "Anomalous properties of the band-edge states in large two-dimensional photonic quasicrystals," Phys. Rev. B **76**, 165132 (2007).
35. R. D. Meade, K. D. Brommer, A. M. Rappe, and J. D. Joannopoulos, "Photonic bound states in periodic dielectric materials," Phys. Rev. B **44**, 13772–13774 (1991).
36. E. Yablonovitch, T. J. Gmitter, R. D. Meade, A. M. Rappe, K. D. Brommer, and J. D. Joannopoulos, "Donor and acceptor modes in photonic band structure," Phys. Rev. Lett. **67**, 3380–3383 (1991).
37. A. Yamilov and H. Cao, "Highest-quality modes in disordered photonic crystals," Phys. Rev. A **69**, 031803 (2004).
38. S. G. Johnson and J. D. Joannopoulos, "Block-iterative frequency-domain methods for Maxwell's equations in a planewave basis," Opt. Express **8**, 173-190 (2001), http://www.opticsexpress.org/abstract.cfm?URI=OPEX-8-3-173.
39. K. Busch and S. John, "Photonic band gap formation in certain self-organizing systems," Phys. Rev. E **58**, 3896–3908 (1998).
40. E. Macia, "Physical nature of critical modes in Fibonacci quasicrystals," Phys. Rev. B **60**, 10032–10036 (1999).

#101449 - $15.00 USD Received 11 Sep 2008; revised 17 Oct 2008; accepted 17 Oct 2008; published 30 Oct 2008

41. T. Fujiwara, M. Kohmoto, and T. Tokihiro, "Multifractal wave functions on a Fibonacci lattice," Phys. Rev. B **40**, 7413–7416 (1989).
42. X. Jiang, Y. Zhang, S. Feng, K. C. Huang, Y. Yi, and J. D. Joannopoulos, "Photonic band gaps and localization in the Thue-Morse structures," Appl. Phys. Lett. **86**, 201110 (2005).
43. K. Wang, "Light wave states in two-dimensional quasiperiodic media," Phys. Rev. B **73**, 235122 (2006).
44. P. Sheng, *Introduction to Wave Scattering, Localization and Mesoscopic Phenomena* (Academic, 1995)
45. Y. Akahane, T. Asano, B. S. Song, and S. Noda, "High-Q photonic nanocavity in a two-dimensional photonic crystal," Nature **425**, 944–947 (2003).
46. B. S. Song, S. Noda, T. Asano, and Y. Akahane, "Ultra-high-Q photonic double-heterostructure nanocavity," Nat. Mater. **4**, 207–210 (2005).
47. K. Srinivasan and O. Painter, "Momentum space design of high-Q photonic crystal optical cavities," Opt. Express **10**, 670–684 (2002), http://www.opticsinfobase.org/abstract.cfm?URI=oe-10-15-670.
48. A. Yamilov, X. Wu, X. Liu, R. P. H. Chang, and H. Cao, "Self-optimization of optical confinement in an ultraviolet photonic crystal slab laser," Phys. Rev. Lett. **96**, 083905 (2006).

1. Introduction

An intense theoretical and experimental research effort has been recently devoted to the study of the optical transport, scattering and emission properties of quasi-periodic and deterministic aperiodic photonic structures in one and two dimensions. These efforts can unveil the connection between the spectral properties of aperiodic sequences and the complex optical behavior of the resulting structures, leading to novel design concepts for the control of optical fields in photonic devices. Quasi-crystalline two-dimensional photonic structures (PhQ), e.g. quasi-periodic Penrose photonic lattices, have already been intensively investigated. These studies led to the recent demonstrations of optical pseudo-bandgaps [1, 2], light localization [2-4], focusing [5, 6], spontaneous emission enhancement and lasing [7, 8]. Differently from conventional periodic photonic crystals (PhCs), quasi-periodic photonic structures lack translational invariance but possess a high degree of rotational symmetry, five-fold rotations and over six-fold rotations, which are forbidden in periodic structures. Accordingly, the optical modes supported by PhQ are "extended" modes characterized by a high degree of rotational symmetry [2]. It has also been shown that short-range interactions associated with point group rotational symmetries in photonic quasi-crystals play a major role in the mechanism of the bandgap formation, light localization and focusing [2, 3, 6].

Unlike periodic photonic structures or PhQs, deterministic aperiodic (DA) photonic structures lack both translational and rotational symmetry but display remarkable self-similarity (scale invariance symmetry) in their structural and spectral features. Such structures can be easily generated by arranging dielectric or metal scatterers in a 2D lattice constructed by following fractal inflation rules [9, 10]. Previous studies of one-dimensional (1D) DA structures have revealed their unusual light transport and localization properties. Light localization [11, 12], strong group velocity reduction at pseudo-bandgap frequencies [13], fractal scaling of band-gap regions with omnidirectional reflectance [14], and light emission enhancement at localized modes have been demonstrated [15]. Furthermore, attempts have been made to design photonic gaps and localized states in aperiodic structures using Fourier-based inverse optimization algorithms [16]. However, the optical properties of DA structures still remain largely unexplored. In our recent studies of 2D DA lattices composed of noble-metal nanoparticles we have demonstrated broadband plasmonic resonances spanning the entire visible spectrum due to the excitation of multiple photonic-plasmonic scattering resonances [17]. The formation of optical bandgaps in 2D DA photonic structures composed of either dielectric rods or airholes has also been recently demonstrated [18, 19]. Nevertheless, a general theory connecting the geometrical properties of the aperiodic lattices with their optical properties is still lacking, and represents the main challenge in the field of DA photonic structures. In this paper, we perform a systematic comparative analysis of the optical properties of two types of 2D deterministic aperiodic photonic structures: Thue-Morse and Rudin-Shapiro arrays of high-refractive-index dielectric rods embedded in a low-index host medium (air). In general, aperiodic systems are classified according to the spectral measures of their spatial Fourier transforms [9]. The two structures under study are characterized by

#101449 - $15.00 USD Received 11 Sep 2008; revised 17 Oct 2008; accepted 17 Oct 2008; published 30 Oct 2008

singular-continuous (Thue-Morse) and absolutely-continuous (Rudin-Shapiro) Fourier spectra, respectively [10, 17], and embody the most general manifestations of deterministic aperiodic systems.

Periodic photonic structures based on arrays of dielectric nanorods, with and without structural defects, have been extensively studied theoretically [20]. Owing to recent advances in nanofabrication techniques, several types of nanorod PhCs have been successfully fabricated and characterized. These include GaAs/Al_xO_y sandwich-like structures [21] and silicon-on-insulator nanopillar structures [22]. Waveguiding along linear chains and arrays of nanopillars as well as coupling of nanopillar structures to conventional waveguides have also been demonstrated, both numerically and experimentally [21-23]. Furthermore, it has recently been realized that nanopillar-based structures offer a critical advantage for biosensing and optofluidic applications over more traditional PhC design schemes based on arrays of airholes in high-refractive-index membrane structures. In fact, not only the optical modes supported by nanorod-based PhCs feature higher sensitivity to the changes of the surrounding refractive index [24], but they can also be readily integrated on a planar optical chip which includes optofluidic channels for pumping liquids into the plane of the device [25]. In contrast, little is known on the photonic properties of DA arrays of dielectric nanorods. Recently, we have shown that the optical modes supported by DA nanorod-based structures are better suited for sensing applications than band-edge or defect-localized states in periodic PhCs [26]. In this paper, we will rigorously investigate the bandgap and mode localization properties of DA arrays of dielectric nanorods.

2. Morphology of aperiodic structures and computational methodology

The 2D deterministic aperiodic structures considered in this paper are generated by arranging identical circular dielectric cylinders according to simple deterministic algorithms based on the alternation of 1D aperiodic inflation maps along orthogonal directions [10, 17]. This approach uniquely specifies the positions of the dielectric cylinders (blue dots in Fig. 1) in the arrays once the minimum inter-particle separation has been chosen. As a result, the resulting DA photonic structures are long-range correlated, despite their lack of global translational invariance. Thue-Morse arrays (Fig. 1(a)) are generated by a 2D generalization of the aperiodic inflation: $A \rightarrow AB$, $B \rightarrow BA$, where A and B stand for the presence or the absence of a dielectric cylinder or radius r in a unit cell of side length a, respectively [10, 17]. Thue-Morse arrays are characterized by singular-continuous Fourier transforms (Fig. 1(b)), and support optical modes that are neither extended nor exponentially localized. Such modes, dubbed critical modes, are field states with a rich self-similar structure, which can exhibit strong spatial fluctuations at multiple length scales [14, 18, 19, 27]. The inflation rule used to generate the Rudin-Shapiro arrays (Fig. 1(c)) can simply be obtained by the iteration of the two-letter inflation as follows: $AA \rightarrow AAAB$, $AB \rightarrow AABA$, $BA \rightarrow BBAB$, $BB \rightarrow BBBA$. Rudin-Shapiro arrays are characterized by an absolutely continuous (flat) Fourier spectrum (Fig. 1(d)), which makes this DA structure akin to purely random structures or white noise stochastic processes. There is presently no complete agreement on the spectral and localization character of the Rudin-Shapiro eigenmodes. However, it has been recently realized that extended states can coexist with exponentially-localized ones, similar to the field states formed in random structures in the regime of Anderson localization [19, 26, 28-30]. In this paper, we accurately study the light scattering properties of DA structures in two spatial dimensions, and discuss the origin of their optical modes.

In the 2D formulation of the electromagnetic scattering problem for 2D arrays, the polarizations of electromagnetic waves decouple, and two independent scalar problems need to be solved for transverse-electric (TE, electric field in the plane of the array) and transverse-magnetic (TM, electric field normal to the array plane) waves. In the following sections, we will only consider the TM polarization case since rod-based photonic structures always favor the formation of TM bandgaps [1, 20]. In our numerical simulations, we use an efficient algorithm based on the rigorous solution of the 2D scattering and eigenvalue problems in the framework of the generalized multiparticle Mie theory. The technique makes use of Bessel-

#101449 - $15.00 USD Received 11 Sep 2008; revised 17 Oct 2008; accepted 17 Oct 2008; published 30 Oct 2008

Fourier multipolar expansions of electromagnetic fields, and gives an essentially exact solution to the scattering problem, provided that the final matrix equation is truncated at a sufficiently high multipolar order [31-33].

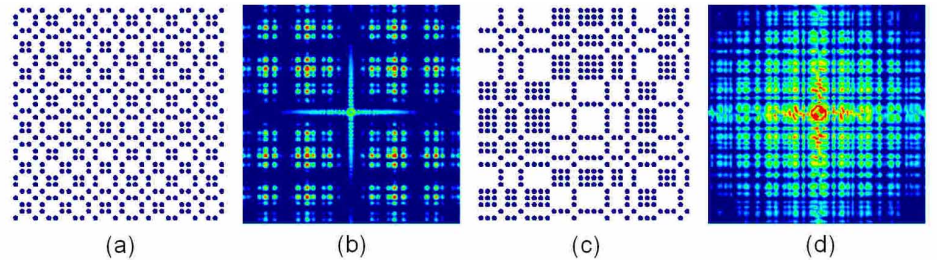

Fig. 1. Real-space lattices of Thue-Morse (a) and Rudin-Shapiro (c) 2D photonic structures and their corresponding reciprocal space representations (lattice Fourier spectra) (b,d).

To study the frequency response of DA photonic structures and to identify the spectral positions of photonic bandgaps, we calculate the radiation power spectrum of a line source embedded in the structure. The total power radiated from the source-array system is evaluated by integrating the output energy flux through a closed contour surrounding the structure [26, 33, 34]. In our simulations, the line source is always placed in the center of the lattice. However, we notice that the frequency locations and spectral widths of the calculated bandgaps do not depend on the choice of the source coordinates. We normalize the total radiated power to the corresponding power emitted by a source in free space. In the case of infinite photonic structures, the source radiation at the frequencies within the photonic bandgap is completely suppressed. For finite-size photonic lattices, the photonic bandgaps are manifested as frequency regions with strongly suppressed radiated power. Outside of the bandgap regions, the values of normalized radiated power fluctuate around unity, and their abrupt (smooth) variations correspond to the excitation of high(low)-quality factor (Q) optical modes in the photonic structure.

3. Bandgap formation and spectral properties of resonant modes

We consider 2D finite-size photonic structures composed of N parallel non-overlapping dielectric rods of radii r and permittivity $\varepsilon = 10.5$ arranged according to Thue-Morse and Rudin-Shapiro aperiodic sequences with the smallest center-to-center separation a ($0 < r/a < 0.5$). The formation of TM bandgaps in several types of nanorod-based PhQ [1-7] and DA structures [18, 19, 26] has already been demonstrated. As previously observed, the spectral positions of low-frequency bandgaps in nanorod-based PhQs largely depend on the resonant properties of the individual rods. As a result, they approximately coincide with the positions of bandgaps in periodic PhCs with matching geometrical and material parameters [1]. Here, we calculate the frequency spectra of the power radiated by a TM-polarized line source embedded in the periodic square-lattice, Thue-Morse and Rudin-Shapiro nanorod-based photonic structures. The results are presented in Figs. 2(a)-(f) . The investigated photonic structures are composed of $N = 100$ (periodic), $N = 128$ (Thue-Morse) $N = 120$ (Rudin-Shapiro) cylinders, respectively. Four types of arrays with progressively larger values of r/a ratios are considered: $r/a = 0.2$ (black lines), $r/a = 0.25$ (red lines), $r/a = 0.3$ (blue lines), and $r/a = 0.35$ (green lines). One photonic bandgap can be identified in the radiated power spectra of the structures with $r/a = 0.2$ and $r/a = 0.25$, while the spectra of the structures with $r/a = 0.3$ and $r/a = 0.35$ feature two bandgaps in the considered frequency range. The values of the dielectric filling fractions (the ratios of the surface area covered by the higher refractive-index dielectric to the total area of the photonic structure) of the aperiodic structures are much lower than corresponding values for the periodic PhC for all the

#101449 - $15.00 USD Received 11 Sep 2008; revised 17 Oct 2008; accepted 17 Oct 2008; published 30 Oct 2008

considered r/a ratios (e.g., $f_{0.2}^{per}=14.2\%$, $f_{0.2}^{TM}=6.8\%$, $f_{0.2}^{RS}=6.4\%$; $f_{0.35}^{per}=40.9\%$, $f_{0.35}^{TM}=20\%$, $f_{0.35}^{RS}=18.7\%$). Nevertheless, it can be seen in Fig. 2 that the spectral positions of the photonic bandgaps are nearly the same for all the structures characterized by identical r/a values. This confirms that, similarly to the case of periodic and quasi-periodic PhCs, the bandgap formation mechanism in DA nanorod-based structures is governed by the Mie-resonances of the individual nanorods. As shown Fig. 2, DA structures feature, in addition to band-edge states, a number of optical modes with resonant frequencies located within the photonic bandgaps. These localized optical modes originate from multiple scattering resonances in aperiodic environments with multiple scale correlations, as reflected by the self-similar diffusive character of their reciprocal (Fourier) spectra (Fig. 1b,d) [9]. From Fig. 2(c,d) and Fig. 2(e,f) we conclude that the number and spectral positions of resonant modes (peaks) depend on the dielectric filling fraction of the aperiodic lattices. In the DA lattices with large dielectric filling fractions, "shallow" modes with frequencies close to the lower-frequency band-edge are formed in the first bandgap. When the dielectric filling fraction is decreased, the modes shift towards the center of the bandgap, and the number of states within the bandgap increases.

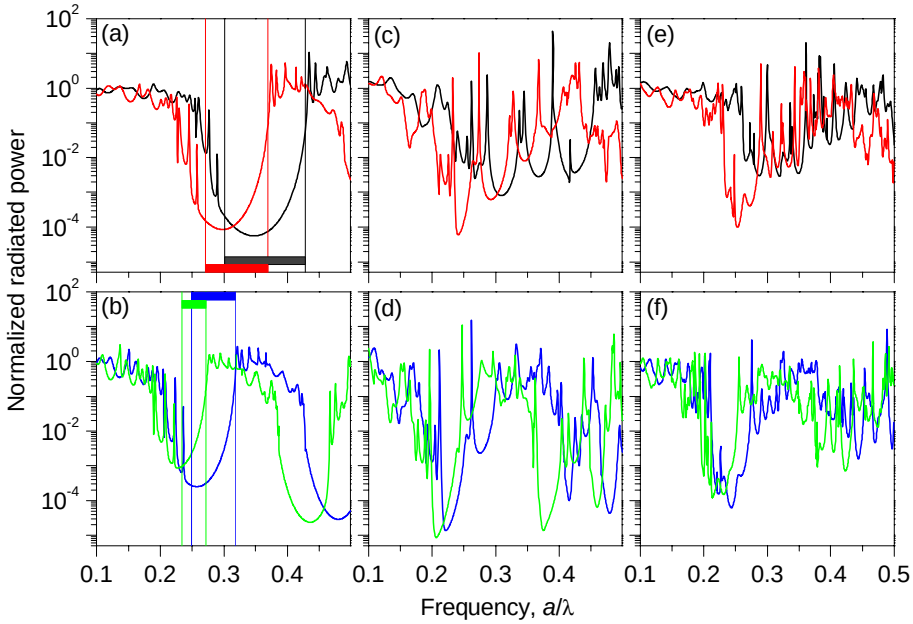

Fig. 2. The radiation power spectra of a TM-polarized line source located in the center of (a,b) a periodic square lattice, (c,d) Thue-Morse lattice and (e,f) Rudin-Shapiro lattice of dielectric cylinders with N^{P}=100, N^{TM}=128, N^{RS} =120, ε=10.5, r/a=0.2 (black lines), r/a=0.25 (red lines), r/a=0.3 (blue lines), and r/a=0.35 (green lines) in air. Spectral positions of the first bandgaps of infinite square-lattice periodic PhCs with matching parameters are indicated with vertical lines and horizontal bars in (a,b).

It is well-known that localized states can also be formed in the bandgaps of periodic PhCs by introducing structural defects [35]. These localized states are classified as either donor or acceptor modes. Donor modes are pulled from the higher-frequency air (conduction) band by introducing extra dielectric material at the defect site. Acceptor modes are pushed into the optical gap from the lower-frequency dielectric (valence) band when dielectric material is removed from one or several unit cells [35, 36]. In general, the spatial electric field distributions for donor and acceptor modes differ substantially. The electric field vector of localized donor modes is prevalently confined in the high refractive index regions of the

#101449 - $15.00 USD Received 11 Sep 2008; revised 17 Oct 2008; accepted 17 Oct 2008; published 30 Oct 2008

structure, while localized acceptor fields are spatially confined in the regions of lower refractive index. We discovered that this behavior is substantially more complex for DA structures. This becomes evident when we realize that DA structures can equivalently be generated by the deterministic removal of cylinders at specified positions of an underlying periodic square-lattice. The lattice constant of the underlying periodic lattice defines the minimum nearest-neighbor distance in the resulting DA structure. This generation methodology helps clarifying the physical nature of critical optical modes in general DA structures. In fact, these deterministic removal processes, result, at each generation step, in the creation of inhomogeneously distributed sub-clusters of dielectric cylinders where interacting (coupled) filed states become localized. The complex electromagnetic interaction among these "construction-induced" defect states, which we call component modes, is responsible for the formation of critical states in DA structures.

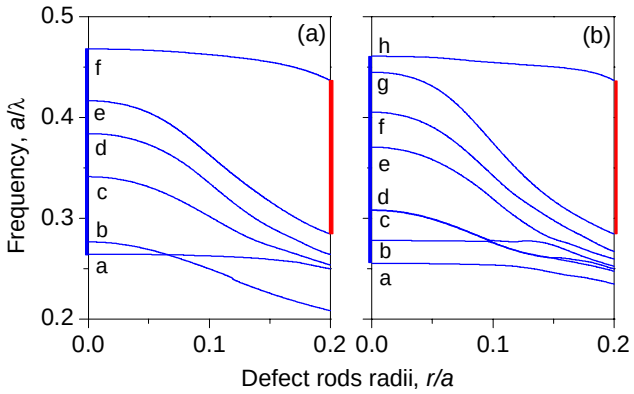

Fig. 3. The evolution of optical component mode frequencies associated with the transformation of the periodic PhC into aperiodic structures by reducing the radii of the rods at the positions determined by the aperiodic sequences. Defect rods radii of r/a=0.2 correspond to a square-lattice periodic PhC with N^{P}=64, and r/a=0 correspond to the Thue-Morse (a) and Rudin-Shapiro (b) aperiodic photonic structures with N^{TM}=N^{RS}=32. The frequency ranges of the first TM bandgaps of the periodic and aperiodic lattices are shown as red and blue sidebars, respectively.

As an example, Fig. 3 shows the formation of optical modes inside the first bandgap of small-size Thue-Morse and Rudin-Shapiro structures composed of 32 cylinders. Both these DA structures can be created by removing cylinders from a periodic 8×8 square-lattice PhC. In Fig. 3, the radii of the rods located at the positions determined by the aperiodic sequences are kept constant, while the radii of all other rods are gradually reduced until they become zero. As we already mentioned, this operation is equivalent to the introduction of multiple structural defects, or component modes, in a periodic square lattice. It can be clearly seen that, as the defect rods radii are decreased, several component modes are pushed into the bandgap from below the dielectric band edge. The modes in Fig. 3(a) and Fig. 3(b) are labeled with letters, and their electric field distributions are shown in Fig. 4 and Fig. 5, respectively. We notice that all the modes formed inside the bandgaps of the Thue-Morse and Rudin-Shapiro structures can be classified as acceptor ones [35, 36]. In addition, we observe that the upper-band-edge mode of the periodic PhC experiences a moderate frequency shift and is mapped into the band-edge mode of an aperiodic structure. On the other hand, the lower-band-edge mode shifts dramatically and maps into one of the acceptor modes. It is also evident from Fig. 3 that the photonic bandgaps of the Thue-Morse and Rudin-Shapiro structures (shown as blue vertical bars in Fig. 3) are wider than the bandgap of the underlying periodic PhC (vertical red bars in Fig. 3). This is a result of their higher degree of structural disorder described by singular-continuous and absolutely continuous Fourier spectra, respectively. The gaps of the DA structures are also shifted towards lower frequencies, in perfect agreement with previous

#101449 - $15.00 USD Received 11 Sep 2008; revised 17 Oct 2008; accepted 17 Oct 2008; published 30 Oct 2008

observations of bandgap positions in 2D quasi-periodic and aperiodic structures [3, 18]. This behavior of the bandgap width and band-edge spectral position originates from long-range optical interactions and multiple-scattering processes occurring in aperiodic and quasi-periodic photonic structures, which are characterized by dense Fourier spectra [3].

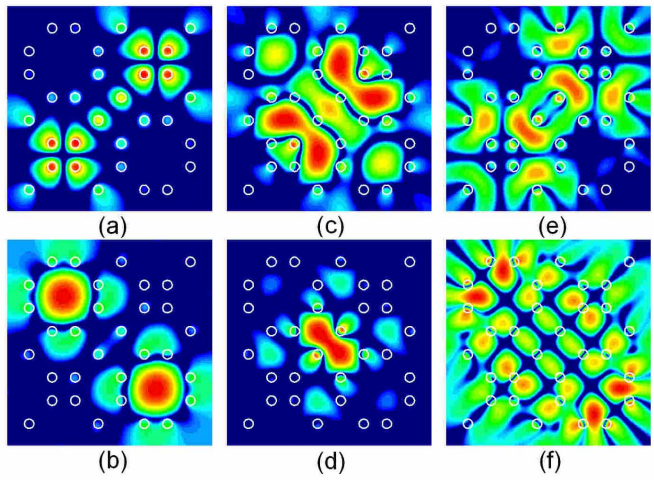

Fig. 4. Electric field patterns ($|E_z|$) of the band-edge and acceptor modes in the first TM bandgap of the Thue-Morse structure with N^{TM}=32: (a) a/λ=0.264; (b) a/λ=0.276; (c) a/λ=0.341; (d) a/λ=0.384; (e) a/λ=0.417; (f) a/λ=0.468.

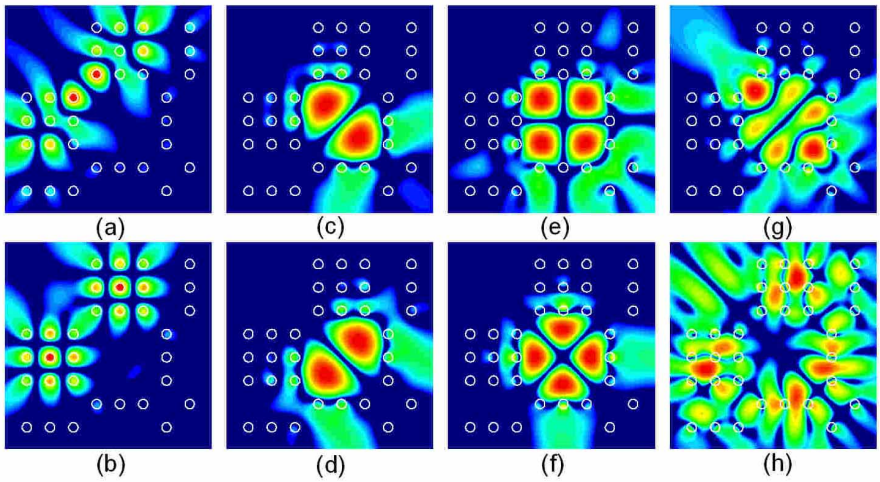

Fig. 5. Electric field patterns ($|E_z|$) of the band-edge and acceptor modes in the first TM bandgap of the Rudin-Shapiro structure with N^{RS}=32: (a) a/λ=0.255; (b) a/λ=0.278; (c) a/λ=0.307; (d) a/λ=0.308; (e) a/λ=0.370; (f) a/λ=0.405; (g) a/λ=0.445; (h) a/λ=0.461.

We also notice that a similar picture for the evolution of the optical modes from the band-edge region to the center of the bandgap has been observed when introducing a progressively larger degree of randomness in a periodic photonic structure [37]. However, differently from the case of random structures, the spectral positions of all the resonant peaks in DA structures are reproducible and deterministic, enabling a higher degree of control on their optical spectra (only limited by fabrication errors). In DA structures, the number of modes and their spectral characteristics can be carefully designed by the proper choice of the geometrical and material parameters of the lattice. Therefore, DA photonic structures bear a large potential for the

#101449 - $15.00 USD Received 11 Sep 2008; revised 17 Oct 2008; accepted 17 Oct 2008; published 30 Oct 2008

engineering of novel photonic components, such as aperiodic lasers with reproducible and controllable emission properties.

We will now investigate how the spectral positions of the optical modes supported by DA photonic structures depend on the size of the structure. Infinite periodic square-lattice PhCs with the same parameters as the structures considered above show bandgaps for TM-polarized modes in the following frequency ranges: $a/\lambda = (0.301 \div 0.428)$ for $r/a = 0.2$; $a/\lambda = (0.271 \div 0.369)$ for $r/a = 0.25$; $a/\lambda = (0.249 \div 0.318)$, $(0.443 \div 0.528)$ for $r/a = 0.3$; and $a/\lambda = (0.234 \div 0.272)$; $(0.399 \div 0.465)$ for $r/a = 0.35$ (position of the first bandgap is marked with colored vertical lines and horizontal bars in Fig 2(a)) [38]. As shown in Fig. 2(a), the widths of the bandgaps of infinite-size and finite-size PhCs do not coincide. Such a shift of the band-edge mode frequencies with the change of the structure size has been previously observed in finite-size periodic and quasiperiodic photonic structures [34]. In periodic PhCs, the shift of the band-edge states is smooth, while PhQs display an abrupt and irregular evolution of the band-edge states as the lattice size is varied [34].

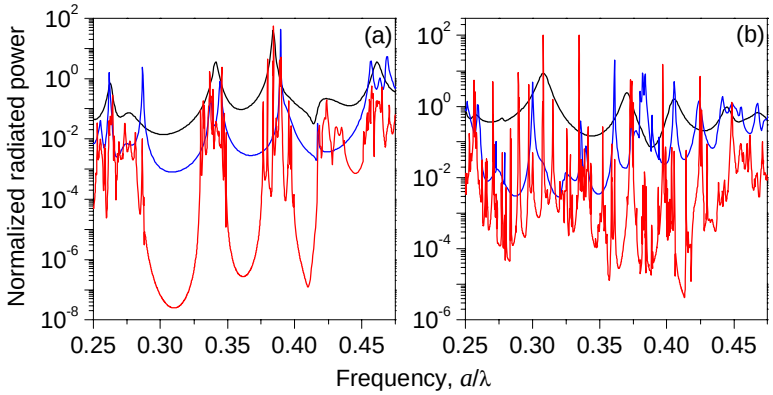

Fig. 6. The radiation power spectra of a TM-polarized line source located in the center of (a) Thue-Morse and (b) Rudin-Shapiro lattice of dielectric cylinders (ε=10.5, *r*/*a*=0.2) in air. Three cluster sizes are considered for each aperiodic structure: $7a \times 7a$, $N^{TM} = N^{RS} = 32$ (black); $15a \times 15a$, $N^{TM} = 128$, $N^{RS} = 120$ (blue); and $31a \times 31a$, $N^{TM} = N^{RS} = 512$ (red).

In Fig. 6, the radiation power spectra in the vicinity of the first TM bandgap of the Thue-Morse and Rudin-Shapiro lattices are plotted for three different structure sizes: $N_1 \sim 30$, $N_2 \sim 120$ and $N_3 \sim 500$. It can be seen that for both DA structures the increase of the structure size induces a damping of the radiated power for the frequencies inside the band gap. Furthermore, new states appear inside the bandgap when the structure size is progressively increased. The linewidths of these modes become narrower, which indicates the increase of the corresponding mode Q-factors. However, two different scenarios for the emergence of new modes within the bandgaps and at the band-edges in Thue-Morse and Rudin-Shapiro structures can be identified. In the optical spectrum of the Thue-Morse structure, new resonances appear both at the band-edges and inside the bandgap (Fig. 6(a)). In addition, by increasing the structure size the band-edge states are shifted toward the bandgap region following an irregular pattern similar to the scenario observed in quasiperiodic photonic structures [34]. However, the photonic bandgap regions remain always pronounced in 2D Thue-Morse structures of large size (see also [18]). The formation of new modes inside the bandgap occurs due to the splitting of coupled modes originating from repeated local structural elements when increasing the size of Thue-Morse lattices. The resonant frequencies of the new modes are distributed around the spectral positions of the modes supported by smaller-sized structures, and are responsible for the formation of several adjacent bandgaps separated by distinct narrow transmission regions. A similar bandgap scaling, which shows a

#101449 - $15.00 USD Received 11 Sep 2008; revised 17 Oct 2008; accepted 17 Oct 2008; published 30 Oct 2008

remarkable self-similar (fractal) character inherited from the fractality of the construction rule, has previously been demonstrated in 1D Thue-Morse aperiodic structures [14].

On the contrary, in the case of Rudin-Shapiro structures (Fig. 6(b)), a size increase results in the formation of new modes. These modes have resonant frequencies at different positions inside the bandgap, reflecting the appearance of novel local structural patterns, which spring at each scaling generation in aperiodic environments with flat spatial (Fourier) spectra. The frequency positions of the sharp resonant modes in Rudin-Shapiro structures are uniquely defined by the structure design, unlike the positions of the optical modes formed in random structures. In the limit of an infinite structure, the optical mode spectrum of Rudin-Shapiro structures collapses into a dense set of high-Q states, and no well-defined bandgap regions can be identified. The sharp resonant peaks observed in the spectra of Fig. 6(b) are well isolated in frequency, reflecting the high Q-factors of the corresponding modes and the rapid frequency variations of the optical density of states. Note that large fluctuations of the density of states in photonic structures, even in the absence of a bandgap region, provide a "colored vacuum" for a variety of quantum optical experiments [39]. The absence of a bandgap has also been previously observed in traditional periodic PhC with large degree of structural disorder [37]. However, for periodic structures, an increase in structural disorder is accompanied by a sharp decrease in the Q-factors of localized modes.

4. Localization properties of optical modes

Two-dimensional DA photonic structures provide novel platforms for realizing and investigating various regimes of light localization on chip-size optical devices. In order to reveal the localization properties of the optical modes supported by DA photonic structures, we have investigated the scaling behavior of their near-field distributions with increasing structure size. As we already pointed out, DA structures can support both extended and non-extended (quasi-localized or critical) optical modes. Unlike defect modes in periodic PhCs, where light localization is induced by a local symmetry perturbation of the underlying lattice, critically localized modes are formed in DA lattices without introducing structural defects. Owing to the presence of many non-equivalent local arrangements of cylinders (sub-clusters) in DA structures, the properties of critically-localized eigenstates are more complex than those of defect modes in periodic PhCs, and may potentially offer a higher degree of design and tuning flexibility [40].

In Figs. 7 and 8, we plot the near-field intensity distributions of several optical modes supported by large ($N = 512$) Thue-Morse and Rudin-Shapiro photonic structures, respectively. The figures reveal great variability in localization properties of different critical modes, depending on the Fourier properties of the DA lattice and the modes spectral positions. This result is in agreement with previous studies on critical eigenstates in 1D quasiperiodic electronic and photonic structures [40-42]. Based on our systematically computational analysis, several general conclusions on the localization character of critical optical modes in DA structures can be made. First, the field distributions of the eigenstates at the edges of the photonic bandgap of Thue-Morse structures show self-similar spatial patterns (as shown in Fig. 7(a) and Fig. 7(d)) and resemble cluster-periodic states with strong local field amplitude variations (see also similar data for the band-edge states in 1D Thue-Morse structures [42]). These band-edge modes are less localized than the modes with frequencies located in the narrow transmission regions inside the bandgap of Thue-Morse structures. Accordingly, they have lower quality factors (compare Fig. 7(a,d) and Fig. 7(b,c)). The scaling of the band-edge states with the increase of the size of a Thue-Morse structure is similar to the behavior of the corresponding modes in quasiperiodic photonic lattices [34, 43]. This behavior is induced by the optical coupling between resonances localized on the highly-symmetric local structural patterns (local point-symmetry) which repeat throughout the photonic structure at each scaling generation (e.g., note the evolution of the spatial localization of the mode shown in Fig. 4(a) into that of the mode of a large Thue-Morse structure presented in Fig. 7(d)).

#101449 - $15.00 USD Received 11 Sep 2008; revised 17 Oct 2008; accepted 17 Oct 2008; published 30 Oct 2008

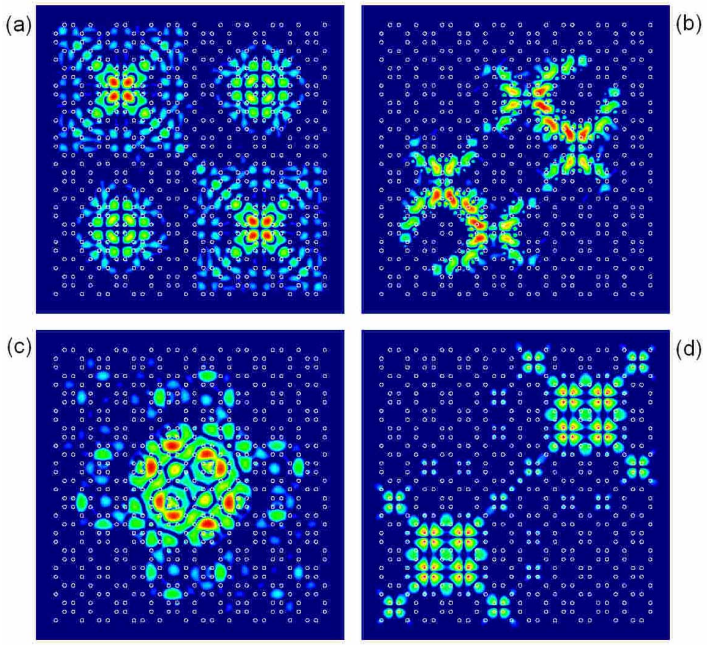

Fig. 7. Electric field patterns ($|E_z|$) of selected critical modes in and around the first TM bandgap of the Thue-Morse structure with N^{TM}=512: (a) a/λ=0.452, Q=8.91×10^2; (b) a/λ=0.417, Q=1.694×10^4; (c) a/λ=0.339, Q=3.363×10^3; (d) a/λ=0.262, Q=8.6×10^2.

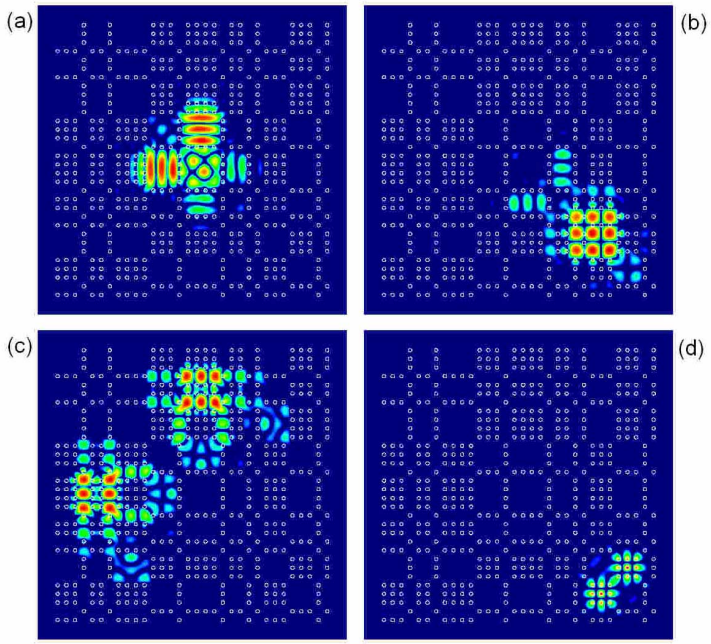

Fig. 8. Electric field patterns ($|E_z|$) of select critical modes in and around the first TM bandgap of the Rudin-Shapiro structure with N^{RS}=512: (a) a/λ=0.397, Q=4.107×10^4; (b) a/λ=0.361, Q=3.002×10^3; (c) a/λ=0.4, Q=3.153×10^4; (d) a/λ=0.279, Q=1.212×10^3.

This situation is substantially different in the case of Rudin-Shapiro structures, as shown in Fig. 8. By comparing Figs. 7 and 8, we notice that the critical modes supported by Rudin-

#101449 - $15.00 USD Received 11 Sep 2008; revised 17 Oct 2008; accepted 17 Oct 2008; published 30 Oct 2008

Shapiro structures are generally more localized than those in the Thue-Morse structures, reflecting the higher degree of structural disorder described by an absolutely continuous Fourier spectrum (Fig. 1(d)). The Rudin-Shapiro eigenstates are also characterized by higher values of Q-factors (narrower mode linewidths). This localization behavior can be explained by the large number of non-equivalent, weakly coupled local configurations (sub-clusters) that exist in the Rudin-Shapiro lattice. As a result, different eigenstates are localized (or rather quasi-localized) in different areas of the structure. Consistently, an increase in the structure size does not have a significant effect on the localization properties of the Rudin-Shapiro modes. For example, the mode pattern presented in Fig. 8(d) is essentially the same as that of the mode supported by the smallest-size Rudin-Shapiro structure (see Fig. 5(b)). The resonant frequency of this mode also experiences a negligible shift with the increase of the structure size. Similarly, the critical mode pattern shown in Fig. 8(b) is already supported by the Rudin-Shapiro structure of the intermediate size ($N = 120$). Our simulations show that an increase in the structure size up to $N = 512$ only weakly affects the field localization character of the optical mode, and results in a small increase of the mode Q-factor (from $Q=1.803\times10^3$ to $Q=3.002\times10^3$) without appreciable shift in the resonant mode frequency. These scaling characteristics of the most localized modes in Rudin-Shapiro structures are analogous to the behavior of exponentially-localized Anderson modes in randomly scattering media [44].

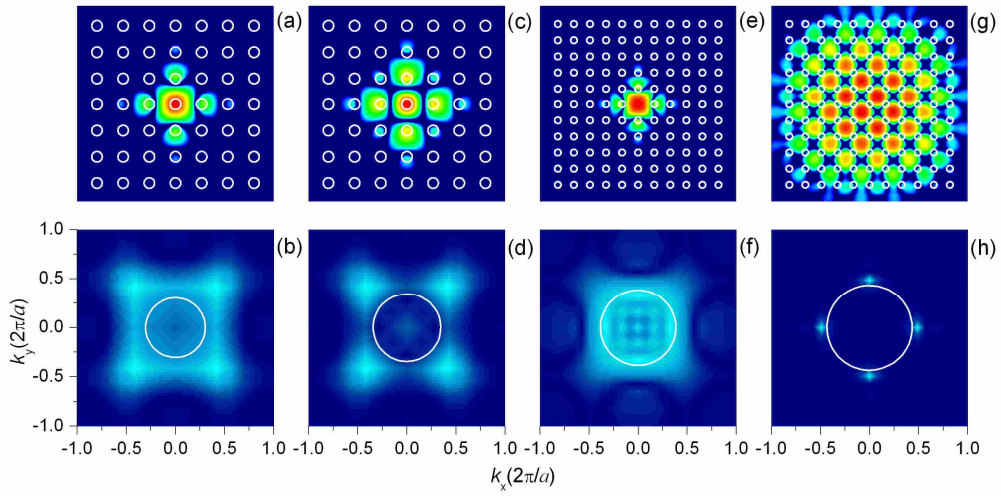

Fig. 9. The electric field profiles ($|E_z|$) of (a) a monopole mode localized in a point defect created in a periodic PhC by reducing the permittivity of a single rod (a/λ=0.2, ε_{rod}=12, ε_{def}=6, a/λ=0.304, $Q=2.618\times10^3$); (c) the same mode, which is delocalized in the plane by reducing the permittivity of the central rod and four neighboring rods (a/λ=0.2, ε_{rod}=12, ε_{def}=6, a/λ=0.345, $Q=2.283\times10^3$); (e) a monopole mode localized in the defect formed by removing the central rod (a/λ=0.2, ε_{rod}=10.5, ε_{def}=1, a/λ=0.384, $Q=5.104\times10^4$); and (g) an extended band-edge mode in a defect-free periodic PhC (a/λ=0.2, ε_{rod}=10.5, a/λ=0.434, $Q=4.51\times10^2$). The corresponding 2D Fourier transform spectra of the modes electric field distributions (b,d,f,h). The areas inside the white circles correspond to the leaky regions.

We notice that our discussion of the localization properties of critical modes in DA photonic structures already suggests a novel approach to suppress vertical radiation losses in three-dimensional (3D) aperiodic structures made of finite-length nanorods [20]. However, in order to better appreciate this important implication, we will first review a general approach (momentum space analysis) for the discussion of the radiation loss balance in photonic structures. It is well known that a monopole acceptor mode that can be formed in a periodic PhC by removing one of the lattice rods is characterized by a very high in-plane optical confinement (high in-plane Q-factor $Q_{\parallel}$) and a very weak out-of-plane confinement (low out-of-plane radiative Q-factor Q_R) [20]. As a result, the overall mode Q-factor

#101449 - $15.00 USD Received 11 Sep 2008; revised 17 Oct 2008; accepted 17 Oct 2008; published 30 Oct 2008

($1/Q = 1/Q_{||} + 1/Q_R$) is severely limited by the vertical field leakage. One of the possible ways to reduce these out-of-plane losses is through the delocalization of the in-plane mode field distribution [20, 45-48]. It is not possible to quantitatively compare the overall quality factors of the modes with various degrees of in-plane localization supported by periodic and aperiodic 3D photonic structures in the frame of the 2D approach used in this study. However, for a qualitative comparison of the vertical confinement properties, we can rely on the momentum-(k)space analysis. This approach is based on the decomposition of the mode electric field into a set of plane-wave components with various **k**-vectors obtained by performing a spatial 2D Fourier transformation of the in-plane mode pattern [45-48]. The plane waves that have the values of the in-plane components of the **k**-vector falling within a circle of diameter $2\pi/\lambda$ (where λ is the light wavelength in air) will leak out of the photonic structure along the vertical direction. We refer to these spatial frequency components as the "leaky components". According to this approach, the localization character of different modes can be compared by looking at the amount of the Fourier components in the leaky region. Several types of the high-Q defect-mode cavity designs have already been proposed using this method [45-47].

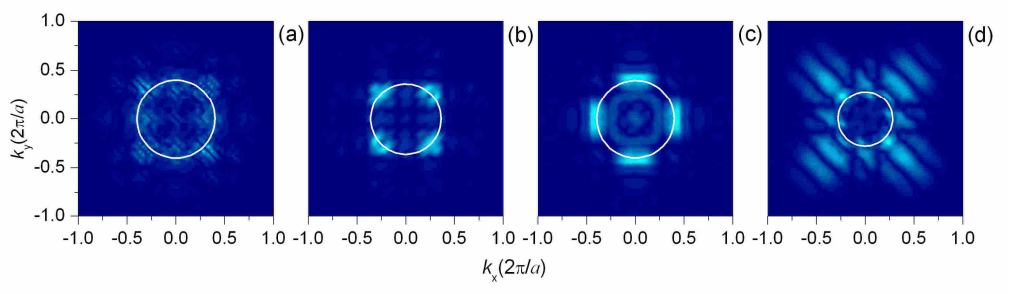

Fig. 10. 2D Fourier transform spectra of the electric field distributions of the critical modes supported by the Thue-Morse structure shown in Fig. 7 (a-d), respectively.

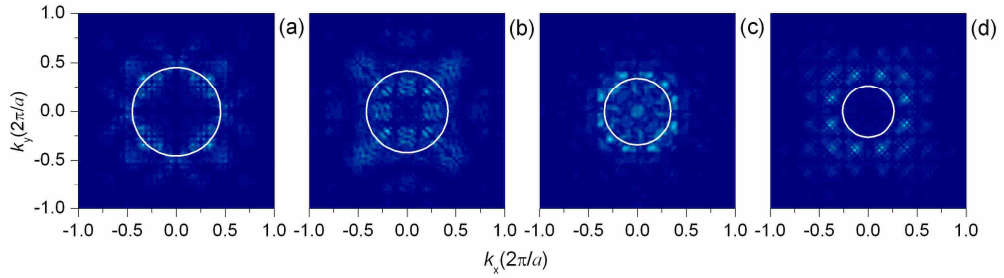

Fig. 11. 2D Fourier transform spectra of the electric field distributions of the critical and localized modes supported by the Rudin-Shapiro structure shown in Fig. 8 (a-d), respectively.

We now apply this method to compare the vertical field confinement properties of several types of modes supported by periodic photonic lattices with and without defects. The first structures to be considered are two defect-mode microcavities formed in a periodic square-lattice PhC by reducing the dielectric constant of either a single rod (Fig. 9(a)) or five neighboring rods (Fig. 9(c)). The Fourier transforms of the two modal field distributions are presented in Fig. 9(b) and Fig. 9(d), respectively. It can be seen that the Fourier spectrum of the more delocalized mode has noticeably smaller components within the leaky region, indicating reduced vertical radiation losses. Indeed, 3D numerical simulations of the out-of-plane radiative Q-factors of these two modes confirm that the five-rod defect mode has an order of magnitude larger Q_R than the single-rod defect one (see [20], chapter 8, Fig. 13). At the same time, our simulations show that the in-plane Q-factor of the delocalized mode is reduced only slightly (Fig. 9). In general, strong localization of the mode field in the plane

#101449 - $15.00 USD Received 11 Sep 2008; revised 17 Oct 2008; accepted 17 Oct 2008; published 30 Oct 2008

results in the broad distribution of its **k**-vector components in the reciprocal space, and thus in larger field leakage in the vertical direction [20]. Clearly, from this point of view, the two extreme cases are a strongly localized point-defect mode (Fig. 9(e)) and a completely delocalized band-edge state (Fig. 9(g)). Consistently, it is well known that the extended band-edge modes have very small out-of-plane radiative losses (see Fig. 9(h)); however, their overall Q-factors are severely limited by the lateral field leakage. In contrast, the strong in-plane localization character of the point-defect mode yields a broad distribution in the momentum space (Fig. 9(f)), which lowers the out-of-plane Q factors, and thus the overall radiative Q-factor.

Based on this preliminary discussion, it is very interesting to investigate now the confinement properties of DA structures, which could offer a novel path to an optimum balance of the radiative losses of confined field states. The momentum space distributions of several critical modes supported by the Thue-Morse and Rudin-Shapiro structures with the in-plane field patterns shown in Figs. 7 and 8 are plotted in Figs. 10 and 11, respectively. Comparing the plots in Figs. 10 and 11 with those in Fig. 9(f) and Fig. 9(h), we can see that the Fourier transform spectra of the critical mode fields show less leaky components than a localized point-defect mode, yet more than an extended band-edge mode (note that the critical modes can have high in-plane Q-factors, comparable with the Q-factor of the point-defect localized mode). This observation confirms the prediction that the delocalized nature of the critical modes in aperiodic photonic structures balances the in-plane and out-of-plane leakage of the modal energy. Note that a similar self-optimization of the light confinement has also been observed in PhCs with structural disorder [48]. Such balancing of horizontal and vertical light confinement in aperiodic structures is expected to result in the increase of the overall critical mode Q-factors, and thus in the reduction of the lasing threshold or in an increase of the spectral resolution of optical sensors based on the excitation of critical modes. Although the critical modes delocalization translates into their larger modal volumes, this is not a disadvantage for some important applications such as e.g., refractive index sensing. In fact, as we have recently demonstrated, the extended nature of critical modes can result in enhanced sensitivity to ambient refractive index variations and thus motivates the development of novel label-free optical biosensors based on DA photonic structures [26].

5. Conclusions

We performed a systematic theoretical study of the spectral and light localization properties of two general types of 2D deterministic aperiodic photonic structures. We discussed the formation of photonic bandgaps in their frequency spectra, and the origin of critically localized optical states. We revealed the differences in the localization and scaling behavior of critical modes in aperiodic lattices with different degrees of spatial correlations, and we have shown that critical modes in DA structures naturally balances in-plane and out-of-plane optical confinement. These results motivate the fabrication of resonant photonic structures with high-Q modes in deterministic aperiodic photonic structures. We expect that the design of deterministic aperiodic optical structures with optimally-balanced high-Q field states and controllable localization properties can have a significant impact on the engineering and fabrication of active devices such as low-threshold, multi-frequency light-emitting devices and optical sensors.

Acknowledgments

The authors wish to thank Prof. Hui Cao and Prof. Mark Brongersma for stimulating discussions and Prof. Enrico Bellotti for the opportunity to utilize the computer resources available in his laboratory at Boston University. This work was partially supported by the US Army Research Laboratory under the contract numbers W911NF-06-2-0040, and W911 NF-07-1-0618, and by the DARPA *Chemical Communication project* (ARM168).

#101449 - $15.00 USD Received 11 Sep 2008; revised 17 Oct 2008; accepted 17 Oct 2008; published 30 Oct 2008